IEEE Open Journal of Signal Processing

Received 5 September 2023; revised 27 November 2023; accepted 30 November 2023. Date of publication 6 December 2023; date of current version 29 December 2023. The review of this article was arranged by Associate Editor Shaofeng Zou.

Digital Object Identifier 10.1109/OJSP.2023.3340111

On Minimizing the Probability of Large Errors in Robust Point Cloud Registration

AMIT EFRAIM AND JOSEPH M. FRANCOS (Senior Member, IEEE)

Department of Electrical and Computer Engineering, Ben Gurion University, Beer Sheva 84105, Israel

CORRESPONDING AUTHOR: AMIT EFRAIM (email: efraimam@post.bgu.ac.il).

This work was supported by Israel Innovation Authority under Grant 77887.

ABSTRACT In solving a model fitting problem, the existence of outliers in the set of measurements can have a devastating effect on the solution accuracy. Traditionally, in order to overcome this problem, robust point cloud registration algorithms are composed of transformation hypothesis generation, followed by hypothesis evaluation aimed at selecting the best hypothesized estimate. Hypotheses evaluation is commonly performed using the sample consensus criterion. However, since this criterion accounts only for the consensus size, it fails when the maximal sample consensus is incorrect. We propose a new hypothesis evaluation approach, generalizing the sample consensus approach, where instead of the sample consensus, the transformation that maximizes the point clouds feature correlation is selected as the best hypothesis. The feature vector at each point contains information such as on local geometry and semantic context. Utilizing this information in the hypotheses evaluation and selection procedure allows for a correct decision even when the hypothesis yielding the maximal sample consensus is false. Consequently, the probability of selecting the correct model increases. We show both mathematically and empirically that substituting the sample consensus criterion with the proposed point cloud feature correlation hypothesis test (PC-FCHT) lowers the probability of large registration errors, compared to using the special case of sample consensus. The proposed PC-FCHT is applicable to any algorithm that follows the hypothesis generation and evaluation scheme, potentially improving the success rates of a wide family of point cloud registration algorithms.

INDEX TERMS Hypothesis evaluation, point clouds, registration, robust estimation.

I. INTRODUCTION

Registration of point cloud measurements of 3D objects has been an active research subject with a vast range of applications in computer vision, robotics, autonomous navigation, and more. A point cloud $\mathcal{P}$ is a finite set of points in $\mathbb{R}^3$. In many applications, these points are samples from a physical object, $\mathcal{O} \subset \mathbb{R}^3$ (we may think of it as a surface in 3D). Viewing point clouds as sets of samples, the registration problem may be formulated as follows: Let $\mathcal{O} \subset \mathbb{R}^3$ be a 3D object. Let $\mathcal{P}$ and $\mathcal{Q}$ be two differently sampled, partially overlapping point cloud observations on $\mathcal{O}$ related by an unknown rigid transformation $T_0 \in \mathrm{SE}(3)$ such that $\mathcal{P} \subset \mathcal{O}$ is a sampled observation on $\mathcal{O}$ and $\mathcal{Q} \subset T_0(\mathcal{O})$ is a different sampled observation on the object after it has undergone a rigid transformation T_0.

When there is no assumption on the initial pose of the models undergoing registration, the most common approach for point cloud registration is the process of matching key points using local geometric features (e.g., [1], [2], [3], [4], [5], [6], [7], [8]), followed by a robust registration algorithm to obtain an approximate alignment (e.g., Random Sample Consensus (RANSAC) [9], TEASER++ [10], Spectral Matching [11], Fast Global Registration [12], Deep Global Registration [13], PointDSC [14], SC^2-PCR [15], and SACF-Net [16]). Once an approximate alignment is obtained, local optimization is usually performed (e.g., [17], [18]).

The robust registration step is essential since the existence of outliers in the available measurements results in large estimation errors. In order to mitigate the devastating effect of the existence of high rates of outliers in the available measurements, robust registration algorithms are designed in accordance with the hypotheses generation and evaluation framework (e.g. [9], [14], [15], [19]): First, multiple hypotheses of the estimated transformation are generated, followed by

evaluation of the hypotheses and selection of the best fitting hypothesis.

The most common approach for hypothesis generation and evaluation is the Random Sample Consensus (RANSAC) algorithm [9]. In RANSAC, a high number of hypotheses is generated by randomly selecting minimal sets of matches to estimate the transformation. Hypothesis evaluation is then performed by maximizing the sample consensus (i.e., the number of estimated inliers). Given two point clouds, $\mathcal{P}, \mathcal{Q} \subset \mathbb{R}^3$ related by a rigid transformation and a set of hypothesized transformations relating them $\mathcal{T} = \{\hat{T}_i\}_{i=1}^N$, the sample consensus decision is defined by

$$\hat{T}_{SC} = \underset{T \in \mathcal{T}}{argmax} \, |\{(p, q) \in \mathcal{P} \times \mathcal{Q} | \, \|T(q) - p\| < \epsilon\}| \quad (1)$$

where ϵ is a parameter determined by the expected accuracy requirement.

Using this approach, significant progress has been achieved in recent years, mainly by improving the quality of local feature descriptors using deep learning [4], [5], [6], [7], [8]). The foregoing hypothesis generation and evaluation steps can be identified in other approaches as well. In Super4PCS [19] for example, hypotheses are generated by matching sets of four co-planar congruent points to obtain transformation estimates, and then, similarly to RANSAC, hypotheses are tested by the size of the consensus set. More recently, deep learning methods for point cloud registration have been proposed (e.g., [13], [14], [20], [21]). PointDSC [14], for example, follows the same pattern where multiple hypotheses are generated using spatial consistency and spectral matching blocks. Then, the best hypothesis is selected based on the size of the corresponding consensus set. SC^2-PCR [15] follows the same pattern, choosing the best hypothesis using the sample consensus criterion. SC^2-PCR++ [22], on the other hand improves the hypothesis selection using feature and spatial consistency constrained truncated Chamfer distance. Using the consensus set size to choose from multiple hypotheses is a common practice and seems to achieve good results in most cases. However, in some cases, such as in the presence of small overlap or repeating patterns, the sample consensus rule is too naive to correctly discriminate between correct and false hypotheses. This is because in these challenging cases, the consensus size associated with the correct hypothesis is not necessarily, the largest (See, Fig. 1 for examples). A major drawback of any sample consensus approach is that regardless of the algorithm's ability to generate accurate hypotheses, if a false hypothesis achieves higher sample consensus than the correct hypothesis, the latter cannot be detected. This, in turn results in overall accuracy and robustness loss, as shown in Section IV.

Thus, we propose that instead of making a decision based solely on Euclidean distances between the assumed matching points (1), a correlation criterion that correlates the geometric and contextual properties of the entire point clouds is to be preferred as it allows to make the correct decision even when the hypothesis that results in the largest sample consensus is false.

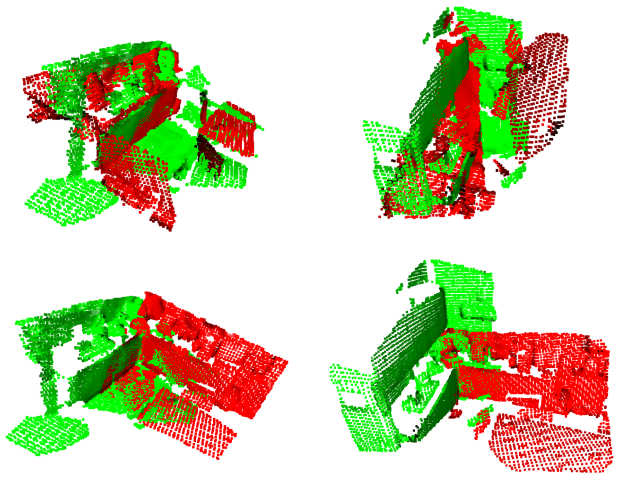

(a) (b)

FIGURE 1. Sample consensus failure cases (Top) compared to successful PC-FCHT (Bottom). It can be seen in the top row that a false solution was generated, with maximal but false sample consensus. In (a), the false solution seems geometrically coherent. Only by utilizing dense features through the PC-FCHT, the correct solution was obtained. In (b), it can be seen that there is only a small overlap between the scans, increasing the probability of a false solution with the largest sample consensus.

The proposed point clouds feature correlation aggregates the inner product of geometric features between point clouds after applying the hypothesized transformation, weighted by the distance between the points. This operation allows for the incorporation of important discriminative information such as local geometry, surface normals, and even semantic context into the hypotheses evaluation. It therefore enables a correct decision even when the consensus size associated with the correct hypothesis is not maximal, which results in an increased probability of making a correct decision. As shown in the experimental part (see, Section IV), the proposed hypothesis evaluation method can be easily integrated into existing methods, replacing the common consensus size criterion, thus resulting in increased robustness and accuracy.

The rest of the paper is structured as follows. In Section II we present the proposed algorithm for hypothesis evaluation. Section III provides formal analysis of the proposed method. In Section IV we present the results of the performed experiments. Finally, in Section V we discuss our conclusions.

II. HYPOTHESIS EVALUATION USING POINT CLOUDS FEATURE CORRELATION

The goal of the proposed Point Clouds Feature Correlation Hypothesis Testing (PC-FCHT) is to determine the best transformation estimate given a set of noisy estimates $\{\hat{T}_i\}_{i=1}^N \in SE(3)$.

Let $F : \mathbb{R}^3 \rightarrow \mathbb{R}^D$ be a function, invariant to rigid transformations, such that it assigns each point in the point cloud a D-dimensional vector. Implementing this function by learned

feature vectors such as D3Feat [7], FCGF [4] or the features proposed in [23], we encapsulate into the vectors global and local contextual information. Define the feature correlation between two point clouds $\mathcal{P} \subset \mathbb{R}^3$ and $\mathcal{Q} \subset \mathbb{R}^3$, as function of an arbitrary transformation $T \in SE(3)$, using features extracted by $F : \mathbb{R}^3 \to \mathbb{R}^D$, as follows:

$$(\mathcal{P} * \mathcal{Q})(T) = \sum_{\mathbf{p} \in \mathcal{P}} k\left(F(\mathbf{p}), F\left(T^{-1}(\mathcal{Q})\right)\right) \tag{2}$$

where k is a weighted correlation function of a single point, defined by

$$k(F(\mathbf{p}), F(\mathcal{Q})) = \sum_{\mathbf{q} \in \mathcal{Q}} w_\sigma(\|\mathbf{p} - \mathbf{q}\|) F(\mathbf{p})^T F(\mathbf{q}) \tag{3}$$

$w_\sigma : \mathbb{R}^+ \to [0, 1]$ is a weight function, inversely related to the distance between given points. In [24], the correlation operator (2) is employed as the reward function to be maximized in a *local* registration framework over the $SE(3)$ manifold, where the goal is to refine an approximate initial transformation estimate. In the current framework, inspired by classic matched filtering (and matched manifold) detection, (2) is employed to *decide* on the best hypothesis among a set of hypothesized transformations in a *global* registration framework.

More specifically, in the proposed method (2) is used to measure the quality of transformation estimates, where the goal is to find the transformation $\widehat{T}_0$ that maximizes (2), instead of the commonly employed consensus size criterion (1). Let $\mathcal{T} = \{\hat{T}_i\}_{i=1}^N$ be a set of hypothesis estimates. The estimate of the underlying transformation T_0 using (2) is given by

$$\widehat{T}_0 = \underset{T \in \mathcal{T}}{argmax} \, (\mathcal{P} * \mathcal{Q})(T) \tag{4}$$

The solution to (4) defines the proposed PC-FCHT.

In the presence of false consensus sets, this approach provides better robustness and accuracy than the standard consensus size criterion. Moreover, the consensus size criterion is shown in Section III to be a special case of the proposed solution, when information regarding the feature vectors associated with the matching points is discarded.

A. INCREASING ROBUSTNESS

In general, the hypotheses generation step creates a finite set of, yet unrefined, hypotheses. Thus in practice, elements in $\mathcal{T}$ do not necessarily fully maximize (2). This, in turn, can lead to (4) choosing a false hypothesis. Thus, to ensure, at a reasonable computational cost, that the chosen hypothesis actually maximizes (2), a second step is performed in order to eliminate false maxima: Instead of simply selecting the hypothesis that maximizes (2), as defined in (4), the K best hypotheses are selected to initialize a second optimization step, where the point clouds correlation is maximized in the proximity of each of the selected estimates using the 3D matched manifold detector over $SE(3)$, derived in [24].

More specifically, the local optimization procedure given by

$$\widehat{T}^{opt} = \underset{T \in \mathrm{SE}(3)}{argmax} \{(\mathcal{P} * \mathcal{Q})(T)\} \tag{5}$$

is repeated for each one of the K best hypotheses, where the hypothesis is employed for initializing the search. The hypothesis achieving the maximal correlation among the K hypotheses after employing (5) is the chosen hypothesis. Thus, let $\mathcal{T}_K \subset \mathcal{T}$ be the set of K hypotheses achieving the highest scores in terms of (2). In addition, denote the optimized hypotheses set as $\mathcal{T}_K^{opt} = \{\widehat{T}_i^{opt}\}_{i=1}^K$, obtained by employing (5) on the estimates in $\mathcal{T}_K$. The estimate of the underlying transformation T_0, given $\mathcal{T}$, is

$$\widehat{T}_0 = \underset{T \in \mathcal{T}_K^{opt}}{argmax} \{(\mathcal{P} * \mathcal{Q})(T)\} \tag{6}$$

This step concludes the proposed feature correlation hypothesis testing (PC-FCHT) method.

III. FORMAL ANALYSIS

In the following, a formal analysis of the PC-FCHT is presented.

A. A SUFFICIENT CONDITION FOR OBTAINING A CORRECT DECISION USING THE PC-FCHT

Proposition 1: Let $\mathcal{P}, \mathcal{Q} \subset \mathbb{R}^3$ be two partially overlapping point clouds, related by a rigid transformation T_0. Denote the overlapping subsets as $\mathcal{P}_O \subset \mathcal{P}$ and $\mathcal{Q}_O \subset \mathcal{Q}$. Assume that each point in $\mathcal{P}_O$ has a corresponding point in $\mathcal{Q}_O$, i.e., $\forall \mathbf{p} \in \mathcal{P}_O$, $\exists \mathbf{q} \in \mathcal{Q}_O$ s.t. $\mathbf{q} = T_0(\mathbf{p})$. In addition, let $F : \mathbb{R}^3 \to \mathbb{R}^D$ be a dense, normalized, feature extracting function, invariant to rigid transformations. Let $C = \mathcal{P} \times \mathcal{Q}$ be the set of all possible correspondences between $\mathcal{P}$ and $\mathcal{Q}$. In addition, let $C_0 = \{(\mathbf{p}, \mathbf{q}) \in C \,|\, \mathbf{q} = T_0(\mathbf{p})\}$ be the correct consensus set found using the ground truth transformation and let $C_1 = \{(\mathbf{p}, \mathbf{q}) \in C \,|\, \mathbf{q} = T_1(\mathbf{p})\}$ be a false consensus set. A decision between T_0 and T_1 is correct if $(\mathcal{P} * \mathcal{Q})(T_0) > (\mathcal{P} * \mathcal{Q})(T_1)$.

Then, a sufficient condition that guarantees a correct decision between T_0 and T_1, using (4), is that $|C_0| > |C_1| \max_{(\mathbf{p},\mathbf{q}) \in C_1} F(\mathbf{p})^T F(\mathbf{q})$.

Proof: For simplicity, assume that $w_\sigma(x) = \mathbb{1}_0(x)$. Then,

$$(\mathcal{P} * \mathcal{Q})(T_0) = \sum_{\mathbf{p} \in \mathcal{P}} \sum_{\mathbf{q} \in \mathcal{Q}} \mathbb{1}_0\left(\left\|\mathbf{p} - T_0^{-1}(\mathbf{q})\right\|\right) F(\mathbf{p})^T F(\mathbf{q}) \tag{7}$$

From the definitions of w_σ and C_0, (7) is equivalent to

$$(\mathcal{P} * \mathcal{Q})(T_0) = \sum_{(\mathbf{p},\mathbf{q}) \in C_0} F(\mathbf{p})^T F(\mathbf{q}) \tag{8}$$

Similarly,

$$(\mathcal{P} * \mathcal{Q})(T_1) = \sum_{(\mathbf{p},\mathbf{q}) \in C_1} F(\mathbf{p})^T F(\mathbf{q}) \tag{9}$$

Because F is invariant to rigid transformations, $F(\mathbf{p}) = F(\mathbf{q})$ $\forall(\mathbf{p}, \mathbf{q}) \in C_0$, and thus since the feature vectors are normalized

$$\sum_{(\mathbf{p},\mathbf{q})\in C_0} F(\mathbf{p})^T F(\mathbf{q}) = \sum_{(\mathbf{p},\mathbf{q})\in C_0} ||F(\mathbf{p})||^2 = |C_0| \tag{10}$$

However, the same does not hold for C_1 in general, and thus

$$\sum_{(\mathbf{p},\mathbf{q})\in C_1} F(\mathbf{p})^T F(\mathbf{q}) \leq \max_{(\mathbf{p},\mathbf{q})\in C_1} F(\mathbf{p})^T F(\mathbf{q}) |C_1| \tag{11}$$

■

Corollary 1: The decision rule (4) enables a correct decision even when $|C_0| < |C_1|$, depending on the extracted features and the ratio of the sizes of the consensus sets.

Proof: The corollary is a direct result of Proposition 1 and the fact that non matching points have different features, i.e., $\max_{(\mathbf{p},\mathbf{q})\in C_1} F(\mathbf{p})^T F(\mathbf{q}) \leq 1$. Clearly, the feasibility of this condition depends on the features' capability to discern different geometric features. ■

Remark: Following Proposition 1, it is concluded that in the case where geometric features are not utilized (i.e., assigning a constant "feature" value to all points), the proposed correlation criterion is reduced to the simple consensus size criterion, where a correct decision is obtained only when $|C_0| > |C_1|$.

In the proof of Proposition 1, a simplifying assumption was made, i.e., the existence of corresponding sampled points in both point clouds: $\forall \mathbf{p} \in \mathcal{P}_O$, $\exists \mathbf{q} \in \mathcal{Q}_O$ s.t. $\mathbf{q} = T_0(\mathbf{p})$. This assumption is not practical, as different scans of the same object will result in different sampling patterns. However, this assumption can be relaxed, as described next.

Proposition 2: Assume each point in $\mathcal{P}_O$ has an approximate corresponding point, such that $\forall \mathbf{p} \in \mathcal{P}_O$, $\exists \mathbf{q} \in \mathcal{Q}_O$ s.t.$\|\mathbf{p} - T_0(\mathbf{q})\| < \epsilon$. Let now

$$C_0 = \{(\mathbf{p}, \mathbf{q}) \in C \mid \|\mathbf{q} - T_0(\mathbf{p})\| < \epsilon\}$$
$$C_1 = \{(\mathbf{p}, \mathbf{q}) \in C \mid \|\mathbf{q} - T_1(\mathbf{p})\| < \epsilon\}.$$

Then, a sufficient condition for a correct decision is

$$|C_0| > |C_1| \frac{\max_{(\mathbf{p},\mathbf{q})\in C_1} F(\mathbf{p})^T F(\mathbf{q})}{\min_{(\mathbf{p},\mathbf{q})\in C_0} F(\mathbf{p})^T F(\mathbf{q})} \tag{12}$$

Proof: The proof follows from the proof of Proposition 1, while changing w_σ to $w_\sigma(x) = \mathbb{1}_{[0,\epsilon)}$. Re-evaluating (8)

$$\sum_{(\mathbf{p},\mathbf{q})\in C_0} F(\mathbf{p})^T F(\mathbf{q}) \geq \min_{(\mathbf{p},\mathbf{q})\in C_0} F(\mathbf{p})^T F(\mathbf{q}) |C_0|. \tag{13}$$

Using (11), we conclude that a sufficient condition for making a correct decision using (4) such that $(\mathcal{P} * \mathcal{Q})(T_0) > (\mathcal{P} * \mathcal{Q})(T_1)$ is that

$$\min_{(\mathbf{p},\mathbf{q})\in C_0} F(\mathbf{p})^T F(\mathbf{q}) |C_0| > \max_{(\mathbf{p},\mathbf{q})\in C_1} F(\mathbf{p})^T F(\mathbf{q}) |C_1| \tag{14}$$

■

B. PROBABILISTIC EVALUATION

In the following, we provide a probabilistic analysis of the hypotheses generation and evaluation procedure. The probability space is defined, followed by a derivation of the conditions required for an algorithm to produce a correct estimate. Then, it is shown that the PC-FCHT has a higher probability of providing a correct estimate, relative to the sample consensus criterion. Since each registration problem and algorithm have their own unique properties, the discussion is limited to a *specific* registration problem, using a *specific* hypotheses generation algorithm, such that the provided analysis results in the evaluation of different hypotheses evaluation tools, given the same set of hypotheses as an input.

Consider a *specific* registration algorithm that generates N hypotheses, in a *specific* registration problem. For example, in RANSAC N hypotheses are generated by randomly sampling N triplets of putative matches. Then, from each triplet, a transformation is estimated, resulting in N transformation hypotheses. In Super4PCS N hypotheses are generated by randomly identifying co-planar sets of four points in one point cloud, followed by finding congruent sets of four co-planar points in the other, and estimating transformations between matching sets of four points. In PointDSC hypotheses are generated by selecting N seeds in the latent space to create N sets of putative matches. From each set, a transformation is estimated using spectral matching. Therefore, the sample set in the probabilistic analysis of such algorithms is the set of all possible outputs of the algorithm, given a registration problem, as described next.

Let $\Omega_{\mathcal{T}_N}$ be the sample set of hypothesis estimates of some registration algorithm, generating N hypotheses for a *specific* registration problem. Each element in $\Omega_{\mathcal{T}_N}$ is a set of N transformation estimates, describing a possible outcome of performing the hypotheses generation step. Each execution of the hypotheses generation step is therefore equivalent to randomly sampling an element from $\Omega_{\mathcal{T}_N}$.

Let $\mathcal{F}_{\mathcal{T}_N}$ denote the event space. The triplet $(\Omega_{\mathcal{T}_N}, \mathcal{F}_{\mathcal{T}_N}, P)$ defines the probability space of a given registration problem, using a given registration algorithm. In the present context, a registration algorithm is characterized by the probability of *both* generating a set of N hypotheses containing at least one correct hypothesis, *and* choosing that hypothesis correctly in the hypothesis evaluation step.

In practice, a correct hypothesis can be defined as any hypothesis that is less than a threshold away from the unknown underlying transformation. Let $d : \mathrm{SE}(3) \times \mathrm{SE}(3) \to \mathbb{R}^+$ be a distance function defined on SE(3), and α a threshold value, determined by the accuracy requirements of the registration problem being solved. Following these definitions, the subset of outcomes that include a correct estimate is given by

$$\mathcal{K} = \left\{ \mathcal{T} \in \mathcal{F}_{\mathcal{T}_N} \middle| \min_{T\in\mathcal{T}} (d(T, T_0)) < \alpha \right\} \subseteq \mathcal{F}_{\mathcal{T}_N} \tag{15}$$

where T_0 is the unknown, underlying transformation. Assuming that the hypothesis evaluation is always correct, the probability of a correct estimation is given by the probability

of sampling a set of hypotheses from $\mathcal{K}$. Since each element in $\mathcal{K}$ is an atom of $\Omega_{\mathcal{T}_N}$

$$P(\mathcal{K}) = \sum_{\mathcal{T}\in\mathcal{K}} P(\mathcal{T}). \tag{16}$$

However, the hypothesis evaluation is not always correct. Therefore, in the following, a generalized probabilistic framework for evaluating registration algorithms is derived, including both the hypothesis generation and evaluation steps. Then, using this framework it is shown that employing the PC-FCHT yields a higher probability of obtaining a correct estimate than the sample consensus:

Let $\mathcal{S} : \mathrm{SE}(3) \to \mathbb{R}$ be a hypothesis evaluation function (e.g., the sample consensus criterion or the PC-FCHT), designed to obtain its maximal value at $\mathcal{S}(T_0)$. However, in some cases, $\mathcal{S}$ may assign a high score to a false hypothesis while a lower score is assigned to T_0, resulting in an erroneous decision. Let $E_{\mathcal{S}}$ be the subset of $\mathcal{K}$ such that among the set of N hypotheses composing each of its elements there is a "misleading" hypothesis $T \neq T_0$, with respect to $\mathcal{S}$, i.e.,

$$E_{\mathcal{S}} = \left\{ \mathcal{T} \in \mathcal{K} \middle| \max_{T\in\mathcal{T}} (\mathcal{S}(T)) > \mathcal{S}(T_0) \right\}. \tag{17}$$

When $E_{\mathcal{S}}$ is not empty $P(\mathcal{K})$ no longer represents the probability of correct estimation since some sets of generated hypotheses contain both a correct hypothesis and an hypothesis that is incorrect but with higher evaluation score. Thus, when considering both the hypothesis generation and evaluation steps, the probability for obtaining a correct *estimate* (as opposed to only a correct hypothesis generation) is given by

$$P(\mathcal{K} \setminus E_{\mathcal{S}}) = \sum_{\mathcal{T}\in\mathcal{K}\setminus E_{\mathcal{S}}} P(\mathcal{T}). \tag{18}$$

Proposition 3: Using the above definitions, given any algorithm that follows the hypothesis generation and evaluation paradigm, the probability of obtaining a correct estimate by employing the PC-FCHT, is higher than the probability of obtaining a correct estimate using the sample consensus criterion.

Proof: Let $E_{SC} \subseteq \mathcal{K}$ be the subset of $\mathcal{K}$ with "misleading" outcomes with respect to the sample consensus criterion, i.e., each element in E_{SC} is a set of N hypotheses with at least one hypothesis $T_1 \neq T_0$, such that $|C_0| < |C_1|$. Similarly, let E_{FC} be the subset of $\mathcal{K}$ with "misleading" outcomes with respect to the PC-FCHT. Following (9), (10) a necessary and sufficient condition for a *false* decision with respect to the PC-FCHT is that

$$|C_0| < \sum_{(\mathbf{p},\mathbf{q})\in C_1} \mathcal{F}(\mathbf{p})^T \mathcal{F}(\mathbf{q})) \tag{19}$$

However,

$$\sum_{(\mathbf{p},\mathbf{q})\in C_1} \mathcal{F}(\mathbf{p})^T \mathcal{F}(\mathbf{q})) \leq \max_{(\mathbf{p},\mathbf{q})\in C_1} \mathcal{F}(\mathbf{p})^T \mathcal{F}(\mathbf{q}) |C_1| \leq |C_1| \tag{20}$$

TABLE 1. Empirical Success Probability of the Sample Consensus and PC-FCHT on 3DMatch Examples

Scene	PC-FCHT	Sample Consensus
redkitchen	0.92	0.56
home_at_scan1	0.89	0.11
home_md_scan9	1.0	0.005
hotel_uc-scan3	1.0	1.0
maryland_hotel1	1.0	0.92
maryland_hotel3	1.0	0.99
mit_76_studyroom	0.714	0.0
mit_lab_hj	0.99	0.31

Thus, the set of hypotheses where $|C_0| < |C_1|$ contains the set of hypotheses where (19) holds, i.e., $E_{FC} \subseteq E_{SC}$. Thus,

$$\mathcal{K} \setminus E_{SC} \subseteq \mathcal{K} \setminus E_{FC} \tag{21}$$

Using (18) and the fact that the comparison is on the same hypotheses generation algorithm and the same problem, it is concluded from (21) that

$$P(\mathcal{K} \setminus E_{FC}) \geq P(\mathcal{K} \setminus E_{SC}) \tag{22}$$

■

IV. EXPERIMENTAL RESULTS

In the experimental section, we provide empirical data to support the advantage of using the proposed PC-FCHT over sample consensus hypothesis evaluation. The tests are performed on the 3DMatch data set [6] for indoor environment, KITTI [25] and NCLT [26] data sets for outdoor environments, and on ModelNet40 [27]. In the performed experiments, it is shown empirically that as expected from Proposition 3, employing the proposed PC-FCHT yields a higher success rate than that of the sample consensus.

A. EMPIRICAL SUCCESS PROBABILITY OF THE SAMPLE CONSENSUS AND PC-FCHT ON 3DMATCH

In this part of the experiments, a single registration problem from each of the 3DMatch data set scenes was used in a Monte Carlo experiment to illustrate Proposition 3. Each registration problem was solved 1000 times as described next. In each iteration, $N = 5000$ hypotheses were generated by randomly selecting different triplets of matches, followed by estimating a transformation from these matches (identical to the initial step of RANSAC). The initial matches were obtained using nearest-neighbor search on FCGF features. Then, the best hypothesis was selected with the proposed PC-FCHT and the sample consensus criterion for comparison.

Table 1 presents the empirical probability of success of the sample consensus and the PC-FCHT methods, evaluated on registration problems from each of the 3DMatch test data set scenes, using the above Monte-Carlo setting. (A correct hypothesis is defined by a rotation error of less than 15° and less than 30 cm.) It is concluded from Table 1 that using

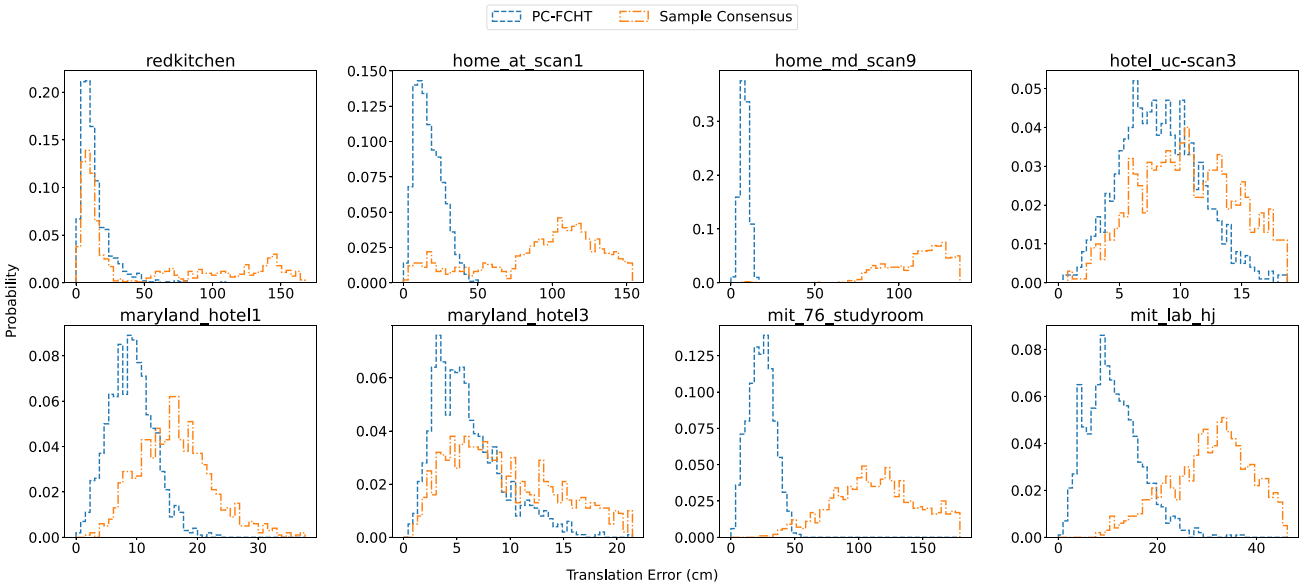

FIGURE 2. **Translation error distribution from Monte Carlo simulations on example registration problems from the 3DMatch data set. 1000 Monte Carlo iterations were executed for each example. On each iteration, hypotheses were generated by randomly sampling 5000 triplets of matching key points, used to generate 5000 hypotheses (the first step of RANSAC). Hypotheses were then selected using either the proposed PC-FCHT or the sample consensus criterion. It is concluded that using the PC-FCHT reduces the probability of large errors compared to the sample consensus criterion.**

the PC-FCHT results in a significantly higher probability of correct decision, as expected from Section III-B.

Fig. 2 depicts the translation error distribution in each example scene. It can be seen that in the examples from *redkitchen*, *home_at_scan1*, *home_md_scan9* and *mit_76_studyroom* the sample consensus was heavily biased towards a false hypothesis, while PC-FCHT results with lower errors.

B. INDOOR REGISTRATION PERFORMANCE

Transformations in the 3DMatch data set problems span a large range: rotations around all axes range between 2° to 178°, with a median of 30°; in 25% of the problems rotations are larger than 45°. Translations range between approximately 2 cm to 4.5 m, with a median of 75 cm; in 25% of the problems translation is larger than 1.5 m. Estimation of large transformations as the ones considered here requires a global registration solution. Accordingly, the baseline methods used for *hypothesis generation* in our comparisons are: PointDSC, 4PCS, and Random selection (RAN in Table 2) which is identical to the random hypothesis generation in RANSAC. In addition, TEASER++ [10] and Spectral Matching [11] are tested as references for the overall accuracy achieved by each of the methods. Three different *dense feature descriptors* were used both for initial matching where applicable, and for the proposed PC-FCHT. These are FCGF [4], D3Feat [7] and FPFH [1]. To evaluate the performance of the PC-FCHT in comparison with the sample consensus, we use the correct hypothesis recall (CHR):

CHR is defined as the percentage of registration problems where a correct hypothesis was chosen by the hypotheses evaluation method, out of those registration problems where at least one of the N generated hypotheses is correct. A correct hypothesis, in this case, is considered as one with rotation and translation estimation errors of less than 15° and 30 cm, respectively, since in this error range, refinement algorithms can be effectively employed to achieve the required high accuracy. In addition, the percentage of registration problems with at least one correct hypothesis generated by each algorithm is also provided and is denoted by CH in Table 2.

To evaluate the overall performance of each approach we evaluate the rotation and translation estimation errors, and the registration recall. We follow standard rotation and translation

TABLE 2. **Performance Comparison Between PC-FCHT and Sample Consensus on the 3DMatch Data Set**

Hypothesis Generation Method	Hypothesis Evaluation Method	CH(%)	CHR(%)	RE(deg)	TE(cm)	RR(%)
PointDSC (FCGF)	SC	96.5	91.0	9.8	25.8	87.8
	PC-FCHT		**96.4**	6.8	18.2	93.0
PointDSC (D3Feat)	SC	95.8	91.3	9.9	27.2	87.5
	PC-FCHT		96.3	6.6	19.2	92.3
PointDSC (FPFH)	SC	82.7	86.9	22.4	58.1	72.0
	PC-FCHT		91.3	21.2	57.2	75.5
4PCS (FCGF)	SC	85.3	46.6	38.5	96.8	39.7
	PC-FCHT		59.3	15.7	45.5	50.5
RAN (D3Feat)	SC	**99.5**	78.3	15.8	41.9	77.9
	PC-FCHT		92.8	6.2	18.0	92.3
RAN (FCGF)	SC	99.4	79.4	14.8	40.25	78.9
	PC-FCHT		94.0	**5.8**	**16.3**	**93.5**
RAN (FPFH)	SC	97.6	71.6	20.8	56.0	69.9
	PC-FCHT		78.3	20.6	54.8	76.5
TEASER (D3Feat)	-	-	-	14.8	40.2	86.8
TEASER (FCGF)	-	-	-	13.2	34.7	88.6
TEASER (FPFH)	-	-	-	34.8	86.7	54.2
SM (D3Feat)	-	-	-	15.9	41.4	81.5
SM (FCGF)	-	-	-	11.6	30.9	86.5
SM (FPFH)	-	-	-	34.8	86.7	54.2

The bold values denote the best performance achieved by the compared methods in each metric.

error definitions [13], [14]: $\text{RE}(\hat{R}) = arccos\frac{tr(\hat{R}R_0^T)-1}{2}$, and $\text{TE}(\hat{\mathbf{t}}) = \|\hat{\mathbf{t}} - \mathbf{t}_0\|$, where R_0 and $\mathbf{t}_0$ denote the rotation and translation components of the ground truth transformation T_0. Registration recall (RR) is defined as the percentage of correct (errors of less than 15° and 30 cm) estimates using the complete registration pipeline. It is important to note that in order to perform a fair comparison, only the output of the hypothesis generation stage was considered in the experiments, excluding any refinement steps that may be applied on top of each of the algorithms. The same set of generated hypotheses was used as input for the sample consensus and PC-FCHT. Table 2 summarizes the results, while example registration problems depicting the failure cases of the sample consensus approach, where the proposed PC-FCHT makes a correct decision are provided in Fig. 1.

Using the results summarized in Table 2, we conclude that with respect to all evaluated hypothesis generation methods and all performance measures, PC-FCHT outperforms the sample consensus as a hypothesis evaluation method. Random hypotheses generation achieves the maximal percentage of registration problems with a correct hypothesis, 99.5%, while PointDSC is only at 96.5%. This high rate of correct hypothesis generation of the Random hypotheses generation, paired with the significantly more accurate identification of the correct hypothesis achieved by PC-FCHT, increases the RR from less than 80% when using sample consensus to 93.5% using PC-FCHT, while reducing translation error from 40 cm to 16 cm. Thus, when Random hypotheses generation employs FCGF-based feature matching and PC-FCHT for hypothesis evaluation, it achieves the best registration recall and accuracy, (better than state of the art PointDSC). Note, however, that indeed when restricting the hypothesis evaluation method to be the (less effective) sample consensus, PointDSC employed using FCGF features performs best, as also reported by [14]. The relatively low CHR in RANSAC (i.e., when using the sample consensus criterion with random hypotheses generation) implies that the bottleneck in performance with RANSAC is indeed the hypothesis evaluation step using the sample consensus.

From the overall lower performance of RANSAC, compared to an identical random hypotheses generation while using PC-FCHT hypothesis evaluation, and given the high CHR with random hypotheses generation, it is concluded that random hypotheses generation achieves a higher rate of generated correct hypotheses, at the cost of higher rate of misleading hypotheses. PointDSC on the other hand, produces a smaller number of hypotheses, with much lower occurrences of misleading hypotheses. By using the PC-FCHT, we were able to utilize the higher rate of correct hypothesis generation of the random generation, resulting in overall better performance.

We therefore conclude that given any registration algorithm that follows the hypothesis generation and evaluation paradigm, the probability of obtaining a correct estimate using the PC-FCHT is higher than the probability of obtaining a correct estimate using the sample consensus criterion.

TABLE 3. Performance Comparison Between PC-FCHT With and Without Correlation Maximization

Hypothesis Generation Method	Correlation Maximization	CH(%)	CHR(%)	RE(deg)	TE(cm)	RR(%)
PointDSC (FCGF)	without	96.3	96.4	6.8	18.2	93.0
	with		**97.1**	6.11	16.2	93.6
PointDSC (D3Feat)	without	95.8	96.3	6.6	19.2	92.3
	with		97.6	5.3	15.5	93.5
PointDSC (FPFH)	without	82.2	91.3	21.2	57.2	75.5
	with		96.1	15.3	42.7	80.0
4PCS (FCGF)	without	77.5	59.3	15.7	45.5	50.5
	with		93.6	7.8	20.5	79.8
RAN (D3Feat)	without	**99.5**	92.8	6.2	18.0	92.3
	with		94.3	**5.06**	**14.9**	93.9
RAN (FCGF)	without	99.4	94.0	5.8	16.3	93.5
	with		94.8	5.2	**14.9**	**94.2**
RAN (FPFH)	without	97.3	78.3	20.6	54.8	76.5
	with		82.6	17.3	47.3	80.6

The bold values denote the best performance achieved by the compared methods in each metric.

C. INCREASING ROBUSTNESS

In Section II-A, we propose an approach to ensure the chosen hypothesis actually maximizes (2), by maximizing the point cloud feature correlation in the proximity of each candidate transformation estimate using the 3D matched manifold detector over $SE(3)$. In Table 3, we provide a comparison between the PC-FCHT with and without the additional correlation maximization step.

It can be seen that both accuracy and success rates were further increased by adding the correlation maximization step. This step is involved with an additional computational load that needs to be taken into account when designing a registration system.

D. OUTDOOR REGISTRATION PERFORMANCE

Outdoor registration performance was evaluated on the KITTI [25] data set using sequences 08-10 and the NCLT [26] data set using sequence "2012-02-04". Registration problems were solved between scans that are approximately 10 m apart in the KITTI data set, and approximately 8 m apart in the NCLT data set. The baseline methods used for hypothesis generation are random hypotheses generation (RAN), which is identical to the random hypotheses generation in RANSAC, and PointDSC [14] (trained only on the KITTI data set), in addition to SM and TEASER++ for reference. Gaussian noise with $\sigma = 0.5 \times$ (mesh resolution) was added to the KITTI data set. Only FCGF features were used. Comparisons are based on translation error (TE), rotation error (RE), and the root mean square error (RMSE) of the distance between corresponding points. The registration RMSE is determined by the known ground truth correspondences as follows (see the definition of C_0 in Proposition 2)

$$\text{RMSE}(\widehat{T}) = \sqrt{\frac{1}{|C_0|}\sum_{(p,q)\in C_0} \left\|\mathbf{q} - \widehat{T}(\mathbf{p})\right\|^2} \tag{23}$$

Table 4 summarizes the results on the KITTI and NCLT data sets. It is concluded that there is a significant gain in

TABLE 4. Rotation Error, Translation Error, and RMSE Averages on the KITTI/NCLT Data Sets

Hypothesis Generation Method	Hypothesis Evaluation Method	RE(deg)	TE(cm)	RMSE(cm)
SM	-	1.3/2.1	33.9/29.5	70.5/57.2
TEASER	-	1.5/1.7	46.0/**27.9**	85.4/57.0
RAN	SC	7.7/8.5	161.4/161.7	278.7/222.2
RAN	PC-FCHT	0.94/**1.6**	15.1/28.2	44.7/**53.5**
PointDSC	SC	1.7/2.6	41.2/43.4	88.0/77.5
PointDSC	PC-FCHT	**0.47**/2.2	**13.7**/34.8	**41.2**/64.0

The bold values denote the best performance achieved by the compared methods in each metric.

TABLE 5. Baseline Evaluation on ModelNet40

Method	RE	TE	CD
PRNet	8.1	0.081	0.00383
RPMNet	1.7	0.018	0.00085
Predator (SC)	1.7	0.019	0.00089
Predator (PC-FCHT)	**1.2**	**0.011**	**0.00072**

The bold values denote the best performance achieved by the compared methods in each metric.

registration accuracy using the PC-FCHT hypothesis evaluation method over the sample consensus. Similarly to the experiments performed on the 3DMatch data set, the largest gain is achieved when using random hypotheses generation. Using the standard random generation approach paired with the PC-FCHT we were able to achieve results comparable to state of the art PointDSC on both the KITTI and NCLT data sets. Note that on the NCLT data set, random generation paired with the PC-FCHT achieved the best results in terms of rotation error and RMSE, thus emphasizing the critical contribution of the proposed PC-FCHT to the overall accuracy of the registration procedure.

E. REGISTRATION PERFORMANCE ON MODELNET40

Following the noisy partial-to-partial variation of ModelNet40, [28], [29], a baseline comparison is performed, comparing the registration performance of PRNet [30], RPMNet [28] and Overlap Predator [31]. Since registration in Overlap Predator is performed using RANSAC, in the presented experiments, hypotheses were randomly generated and then evaluated using either the sample consensus criterion or the proposed PC-FCHT. The features used for the PC-FCHT in these experiments are the dense features generated by [31], weighted by the estimated probability of overlap used in [31] to choose key points from the overlapping regions with a higher probability. Following previous work, we evaluate performance based on the rotation error (RE), translation error (TE), and Chamfer Distance (CD). Table 5 presents the results of the baseline comparison. In addition, two more experiments were performed to further evaluate the robustness of the proposed method. The first is robustness to low overlap, evaluated on ModelLoNet40, [31]. In the second

TABLE 6. Robustness Evaluation on ModelNet40 With Low Overlap and With Added Noise Points, Using Overlap Predator With Random Hypotheses Generation

	ModelLoNet40			Added Noise Points		
Method	RE	TE	CD	RE	TE	CD
SC	5.2	0.132	0.0083	2.1	0.026	0.0109
PC-FCHT	**4.7**	**0.105**	**0.0075**	**1.5**	**0.019**	**0.0106**

The bold values denote the best performance achieved by the compared methods in each metric.

robustness test, 10% of noise points were added to each model (i.e., points that do not exist in the original models). Since in the ModelNet40 registration benchmark, the point clouds are normalized to a unit sphere, random noise points were added such that their (x, y, z) coordinates are normally distributed $\mathcal{N}(0, 0.25^2)$ along each axis. Table 6 presents the results of the robustness evaluation. In the two robustness tests, as well as in the baseline test, employing the proposed PC-FCHT provided the best performance.

V. CONCLUSION

While it is a common practice in existing registration methods to make decisions based on the sample consensus criterion, this approach fails when the maximal sample consensus is associated with a false hypothesis. Thus, instead of utilizing only Euclidean distances between assumed corresponding points, as in the sample consensus, a new hypothesis evaluation approach is proposed: the Point Cloud Feature Correlation Hypothesis Test (PC-FCHT). The proposed method relies on incorporating into the decision mechanism information about the local geometry in the neighborhood of every point, as well as contextual information, by using the point clouds feature correlation. It is concluded that in the case where geometric features are not utilized (i.e., assigning a constant "feature" value to all points), the proposed correlation criterion is reduced to the simple consensus size criterion. Moreover, we show both mathematically and empirically that for any registration algorithm that follows the hypothesis generation and evaluation paradigm, the probability of obtaining a correct estimate using the PC-FCHT is higher than the probability of obtaining a correct estimate using the sample consensus criterion. A limitation of PC-FCHT is that it relies on achieving invariance of the feature vectors to rigid transformations, as well as that its computational complexity is $O(|\mathcal{P}||\mathcal{Q}|D)$, slightly higher than $O(|\mathcal{P}||\mathcal{Q}|)$ of the sample consensus. In practice, however, the increased computational cost of the PC-FCHT is negligible when using parallel GPU computing. The proposed PC-FCHT can be easily integrated into existing registration algorithms, instead of the sample consensus criterion, as has been successfully demonstrated with common registration algorithms in the performed experiments, increasing the accuracy and success rates of these algorithms.

REFERENCES

[1] R. B. Rusu, N. Blodow, and M. Beetz, "Fast point feature histograms (FPFH) for 3D registration," in *Proc. IEEE Int. Conf. Robot. Autom.*, 2009, pp. 3212–3217.

[2] Y. Zhong, "Intrinsic shape signatures: A shape descriptor for 3D object recognition," in *Proc. IEEE/CVF Int. Conf. Comput. Vis. Workshops*, 2009, pp. 689–696.

[3] T. Darom and Y. Keller, "Scale-invariant features for 3-D mesh models," *IEEE Trans. Image Process.*, vol. 21, no. 5, pp. 2758–2769, May 2012.

[4] C. Choy, J. Park, and V. Koltun, "Fully convolutional geometric features," in *Proc. IEEE/CVF Int. Conf. Comput. Vis.*, 2019, pp. 8957–8965.

[5] Z. J. Yew and G. H. Lee, "3Deat-Net: Weakly supervised local 3D features for point cloud registration," in *Proc. Eur. Conf. Comput. Vis.*, 2018, pp. 630–646.

[6] A. Zeng, S. Song, M. Nießner, M. Fisher, J. Xiao, and T. Funkhouser, "3DMatch: Learning local geometric descriptors from RGB-D reconstructions," in *Proc. IEEE Conf. Comput. Vis. Pattern Recognit.*, 2017, pp. 199–208.

[7] X. Bai, Z. Luo, L. Zhou, H. Fu, L. Quan, and C.-L. Tai, "D3Feat: Joint learning of dense detection and description of 3D local features," in *Proc. IEEE/CVF Conf. Comput. Vis. Pattern Recognit.*, 2020, pp. 6358–6366.

[8] S. Horache, J.-E. Deschaud, and F. Goulette, "3D point cloud registration with multi-scale architecture and unsupervised transfer learning," in *Proc. IEEE Int. Conf. 3D Vis.*, 2021, pp. 1351–1361.

[9] M. A. Fischler and R. C. Bolles, "Random sample consensus: A paradigm for model fitting with applications to image analysis and automated cartography," *Commun. ACM*, vol. 24, no. 6, pp. 381–395, Jun. 1981.

[10] H. Yang, J. Shi, and L. Carlone, "Teaser: Fast and certifiable point cloud registration," *IEEE Trans. Robot.*, vol. 37, no. 2, pp. 314–333, Apr. 2021.

[11] M. Leordeanu and M. Hebert, "A spectral technique for correspondence problems using pairwise constraints," in *Proc. IEEE/CVF Int. Conf. Comput. Vis.*, 2005, pp. 148–1489.

[12] Q.Y. Zhou, J. Park, and V. Koltun, "Fast global registration," in *Proc. 14th Eur. Conf. Comput. Vis.*, 2016, pp. 766–782.

[13] C. Choy, W. Dong, and V. Koltun, "Deep global registration," in *Proc. IEEE Conf. Comput. Vis. Pattern Recognit.*, 2020, pp. 2511–2520.

[14] X. Bai et al., "Point DSC: Robust point cloud registration using deep spatial consistency," in *Proc. IEEE Conf. Comput. Vis. Pattern Recognit.*, 2021, pp. 15854–15864.

[15] Z. Chen, K. Sun, F. Yang, and W. Tao, "SC2-PCR: A second order spatial compatibility for efficient and robust point cloud registration," in *Proc. IEEE/CVF Conf. Comput. Vis. Pattern Recognit.*, 2022, pp. 13211–13221.

[16] Y. Wu, X. Hu, Y. Zhang, M. Gong, W. Ma, and Q. Miao, "SACF-Net: Skip-attention based correspondence filtering network for point cloud registration," *IEEE Trans. Circuits Syst. Video Technol.*, vol. 33, no. 8, pp. 3585–3595, Aug. 2023.

[17] P. J. Besl and N. D. McKay, "A method for registration of 3-D shapes," *IEEE Trans. Pattern Anal. Mach. Intell.*, vol. 14, no. 2, pp. 239–256, Feb. 1992.

[18] T. Schmiedel, E. Erik, and H.-M. Gross, "IRON: A fast interest point descriptor for robust NDT-map matching and its application to robot localization," in *Proc. IEEE/RSJ Int. Conf. Intell. Robots Syst.*, 2015, pp. 3144–3151.

[19] N. Mellado, D. Aiger, and N. J. Mitra, "Super 4PCS fast global pointcloud registration via smart indexing," *Comput. Graph. Forum*, vol. 33, no. 5, pp. 205–215, 2014.

[20] G. D. Pais, P. Miraldo, S. Ramalingam, J. C. Nascimento, V. M. Govindu, and R. Chellappa, "3DRegNet: A deep neural network for 3D point registration," in *Proc. IEEE Conf. Comput. Vis. Pattern Recognit.*, 2019, pp. 7193–7203.

[21] Y. Wang and J. Solomon, "Deep closest point: Learning representations for point cloud registration," in *Proc. IEEE/CVF Int. Conf. Comput. Vis.*, 2019, pp. 3523–3532.

[22] Z. Chen, K. Sun, F. Yang, L. Guo, and W. Tao, "SC^2-PCR: Rethinking the generation and selection for efficient and robust point cloud registration," *IEEE Trans. Pattern Anal. Mach. Intell.*, vol. 45, no. 10, pp. 12358–12376, Oct. 2023.

[23] Y. Wu et al., "Self-supervised intra-modal and cross-modal contrastive learning for point cloud understanding," *IEEE Trans. Multimedia*, to be published, doi: 10.1109/TMM.2023.3284591.

[24] A. Efraim and J. M. Francos, "3D matched manifold detection for optimizing point cloud registration," in *Proc. IEEE Int. Conf. Elect., Comput., Commun. Mechatronics Eng.*, 2022, pp. 1–5.

[25] A. Geiger, P. Lenz, and R. Urtasun, "Are we ready for autonomous driving? The KITTI vision benchmark suite," in *Proc. IEEE Conf. Comput. Vis. Pattern Recognit.*, 2012, pp. 3354–3361.

[26] N. Carlevaris-Bianco, A. K. Ushani, and R. M. Eustice, "University of michigan north campus long-term vision and LiDAR dataset," *Int. J. Robot. Res.*, vol. 35, no. 9, pp. 1023–1035, 2015.

[27] Z. Wu et al., "3D shapeNets: A deep representation for volumetric shapes," in *Proc. IEEE Conf. Comput. Vis. Pattern Recognit.*, 2015, pp. 1912–1920.

[28] Z. J. Yew and G. H. Lee, "RPM-Net: Robust point matching using learned features," in *Proc. IEEE/CVF Conf. Comput. Vis. Pattern Recognit.*, 2020, pp. 11824–11833.

[29] Y. Wu, Q. Yao, X. Fan, M. Gong, W. Ma, and Q. Miao, "PANet: A point-attention based multi-scale feature fusion network for point cloud registration," *IEEE Trans. Instrum. Meas.*, vol. 72, pp. 1–13, 2023.

[30] Y. Wang and J. M. Solomon, "PRNet: Self-supervised learning for partial-to-partial registration," in *Proc. Adv. Neural Inf. Process. Syst.*, H. Wallach, H. Larochelle, A. Beygelzimer, F. D' Alché-Buc, E. Fox, R. Garnett and R. A. Rodriguez-Solis, Eds. vol. 32, 2019. [Online]. Available: https://proceedings.neurips.cc/paper_files/paper/2019/file/ebad33b3c9fa1d10327bb55f9e79e2f3-Paper.pdf

[31] S. Huang, Z. Gojcic, M. Usvyatsov, K. Schindler, and A. Wieser, "PREDATOR: Registration of 3D point clouds with low overlap," in *Proc. IEEE/CVF Conf. Comput. Vis. Pattern Recognit.*, 2021, pp. 4267–4276.